

The interpretation of partial Patterson functions and its application to structure analyses of sérandite $\text{Mn}_2\text{NaHSi}_3\text{O}_9$ and banalsite $\text{BaNa}_2\text{Al}_4\text{Si}_4\text{O}_{16}$ *

By Y. TAKÉUCHI, Y. KUDOH and N. HAGA

Mineralogical Institute, Faculty of Science, University of Tokyo, Hongo, Tokyo

(Received 28 August 1972)

Auszug

Ein allgemeines Verfahren zur Zerlegung der Vektorsätze aus zentrosymmetrischen Sätzen von positiven und negativen Punkten wird beschrieben. Die für einen Vektorsatz charakteristischen negativen Bilder können mit Erfolg zur Lokalisierung von Inversionsbildern benutzt werden. Mehrfache Lösungen von Vektorsätzen, die möglichen Typen multipler Bilder entsprechen, werden diskutiert. Das Verfahren kann im allgemeinen zur Deutung partieller Patterson-Funktionen von Überstrukturen angewandt werden, wenn sie aus den Überstruktur-Interferenzen allein berechnet sind. Als Beispiel für die Anwendung wird die Analyse der Strukturen von Serandit und Banalsit, die beide Quasi-Perioden aufweisen, behandelt.

Abstract

A general procedure has been described of decomposing vector sets of centrosymmetrical sets of positive and negative unit points. The negative images which are characteristic of the vector sets can effectively be utilized to locate inversion images. Multiple solutions of the vector sets due to possible types of multiple images are discussed. The procedure can readily be exploited, in general, for the straightforward interpretation of partial Patterson functions of superstructures calculated from superstructure reflections alone.

Examples of applying this procedure have been shown to the structure determinations of sérandite and banalsite, both having strong quasi-periodicities.

Introduction

The partial Patterson synthesis of a crystal based upon its superstructure reflections alone gives the self-convolution of the function $\delta(x) = \rho(x) - \langle \rho(x) \rangle_{\text{subcell}}$, where $\rho(x)$ is the electron density of the crystal, and $\langle \rho(x) \rangle_{\text{subcell}}$ the average of $\rho(x)$ with respect to its subcells. Noting that $\delta(x)$ is a function having negative maxima as well as

* *Dedicated to Professor M. J. Buerger on the occasion of his 70th birthday.*

positive, TAKÉUCHI (1972) has studied the basic geometrical features characteristic of the partial Pattersons in terms of the vector set given by a set of positive and negative unit points. The application of this theory has been shown to the structure determination of $\text{Cu}_7\text{As}_6\text{Se}_{13}$ which has a thirteenfold distortion structure based upon sphalerite (TAKÉUCHI and HORIUCHI, 1972). The present paper describes practical procedures of decomposing vector sets of this specific kind in order to facilitate straightforward application of this method to the solution of superstructures generally.

Since in the above mentioned paper by TAKÉUCHI (1972), basic image properties are discussed mainly for vector sets of non-centrosymmetrical point sets, the present paper will deal with the problem for those of centrosymmetrical point sets. However, the representation of vector sets of centrosymmetrical point sets bears some complexity compared to that of vector sets of non-centrosymmetrical point sets. Therefore, a general representation of vector sets of centrosymmetrical point sets is described first.

Representation of vector sets of centrosymmetrical sets of points

Consider a centrosymmetrical set of points consisting of $2n$ positive points $p_1, p_2, p_3, \dots, p_n, p'_1, p'_2, p'_3, \dots, p'_n$, and $2n$ negative points $\bar{p}_1, \bar{p}_2, \bar{p}_3, \dots, \bar{p}_n, \bar{p}'_1, \bar{p}'_2, \bar{p}'_3, \dots, \bar{p}'_n$. Let p'_i and \bar{p}'_k be the points respectively related to p_i and \bar{p}_k by the center of symmetry in the set. Then the vector-set array of this point set can conveniently be partitioned into four sub-arrays, and expressed by

$$\mathbf{V} = \begin{array}{cc} \mathbf{A}_{pq} & \mathbf{B}_{p'q'} \\ \mathbf{C}_{p'q} & \mathbf{D}_{p'q'} \end{array} \quad (1)$$

The sub-arrays each of which consisting of $2n \times 2n$ images represent the arrays of images as follows:

$$\begin{aligned} \mathbf{A}_{pq} = & \begin{array}{cccccc} p_1 p_1 & p_1 p_2 & \cdots & p_1 p_n & p_1 \bar{p}_1 & p_1 \bar{p}_2 \cdots p_1 \bar{p}_n \\ p_2 p_1 & p_2 p_2 & \cdots & p_2 p_n & p_2 \bar{p}_1 & p_2 \bar{p}_2 \cdots p_2 \bar{p}_n \\ \vdots & & & & & \\ p_n p_1 & p_n p_2 & \cdots & p_n p_n & p_n \bar{p}_1 & p_n \bar{p}_2 \cdots p_n \bar{p}_n \\ \bar{p}_1 p_1 & \bar{p}_1 p_2 & \cdots & \bar{p}_1 p_n & \bar{p}_1 \bar{p}_1 & \bar{p}_1 \bar{p}_2 \cdots \bar{p}_1 \bar{p}_n \\ \bar{p}_2 p_1 & \bar{p}_2 p_2 & \cdots & \bar{p}_2 p_n & \bar{p}_2 \bar{p}_1 & \bar{p}_2 \bar{p}_2 \cdots \bar{p}_2 \bar{p}_n \\ \vdots & & & & & \\ \bar{p}_n p_1 & \bar{p}_n p_2 & \cdots & \bar{p}_n p_n & \bar{p}_n \bar{p}_1 & \bar{p}_n \bar{p}_2 \cdots \bar{p}_n \bar{p}_n \end{array} \end{aligned}$$

$$\mathbf{B}_{pq'} = \begin{matrix} p_1 p'_1 & p_1 p'_2 & \cdots & p_1 p'_n & p_1 \bar{p}'_1 & p_1 \bar{p}'_2 & \cdots & p_1 \bar{p}'_n \\ p_2 p'_1 & p_2 p'_2 & \cdots & p_2 p'_n & p_2 \bar{p}'_1 & p_2 \bar{p}'_2 & \cdots & p_2 \bar{p}'_n \\ \vdots & & & & & & & \\ p_n p'_1 & p_n p'_2 & \cdots & p_n p'_n & p_n \bar{p}'_1 & p_n \bar{p}'_2 & \cdots & p_n \bar{p}'_n \\ \bar{p}_1 p'_1 & \bar{p}_1 p'_2 & \cdots & \bar{p}_1 p'_n & \bar{p}_1 \bar{p}'_1 & \bar{p}_1 \bar{p}'_2 & \cdots & \bar{p}_1 \bar{p}'_n \\ \bar{p}_2 p'_1 & \bar{p}_2 p'_2 & \cdots & \bar{p}_2 p'_n & \bar{p}_2 \bar{p}'_1 & \bar{p}_2 \bar{p}'_2 & \cdots & \bar{p}_2 \bar{p}'_n \\ \vdots & & & & & & & \\ \bar{p}_n p'_1 & \bar{p}_n p'_2 & \cdots & \bar{p}_n p'_n & \bar{p}_n \bar{p}'_1 & \bar{p}_n \bar{p}'_2 & \cdots & \bar{p}_n \bar{p}'_n \end{matrix}$$

$$\mathbf{C}_{p'q} = \begin{matrix} p'_1 p_1 & p'_1 p_2 & \cdots & p'_1 p_n & p'_1 \bar{p}_1 & p'_1 \bar{p}_2 & \cdots & p'_1 \bar{p}_n \\ p'_2 p_1 & p'_2 p_2 & \cdots & p'_2 p_n & p'_2 \bar{p}_1 & p'_2 \bar{p}_2 & \cdots & p'_2 \bar{p}_n \\ \vdots & & & & & & & \\ p'_n p_1 & p'_n p_2 & \cdots & p'_n p_n & p'_n \bar{p}_1 & p'_n \bar{p}_2 & \cdots & p'_n \bar{p}_n \\ \bar{p}'_1 p_1 & \bar{p}'_1 p_2 & \cdots & \bar{p}'_1 p_n & \bar{p}'_1 \bar{p}_1 & \bar{p}'_1 \bar{p}_2 & \cdots & \bar{p}'_1 \bar{p}_n \\ \bar{p}'_2 p_1 & \bar{p}'_2 p_2 & \cdots & \bar{p}'_2 p_n & \bar{p}'_2 \bar{p}_1 & \bar{p}'_2 \bar{p}_2 & \cdots & \bar{p}'_2 \bar{p}_n \\ \vdots & & & & & & & \\ \bar{p}'_n p_1 & \bar{p}'_n p_2 & \cdots & \bar{p}'_n p_n & \bar{p}'_n \bar{p}_1 & \bar{p}'_n \bar{p}_2 & \cdots & \bar{p}'_n \bar{p}_n \end{matrix}$$

$$\mathbf{D}_{p'q'} = \begin{matrix} p'_1 p'_1 & p'_1 p'_2 & \cdots & p'_1 p'_n & p'_1 \bar{p}'_1 & p'_1 \bar{p}'_2 & \cdots & p'_1 \bar{p}'_n \\ p'_2 p'_1 & p'_2 p'_2 & \cdots & p'_2 p'_n & p'_2 \bar{p}'_1 & p'_2 \bar{p}'_2 & \cdots & p'_2 \bar{p}'_n \\ \vdots & & & & & & & \\ p'_n p'_1 & p'_n p'_2 & \cdots & p'_n p'_n & p'_n \bar{p}'_1 & p'_n \bar{p}'_2 & \cdots & p'_n \bar{p}'_n \\ \bar{p}'_1 p'_1 & \bar{p}'_1 p'_2 & \cdots & \bar{p}'_1 p'_n & \bar{p}'_1 \bar{p}'_1 & \bar{p}'_1 \bar{p}'_2 & \cdots & \bar{p}'_1 \bar{p}'_n \\ \bar{p}'_2 p'_1 & \bar{p}'_2 p'_2 & \cdots & \bar{p}'_2 p'_n & \bar{p}'_2 \bar{p}'_1 & \bar{p}'_2 \bar{p}'_2 & \cdots & \bar{p}'_2 \bar{p}'_n \\ \vdots & & & & & & & \\ \bar{p}'_n p'_1 & \bar{p}'_n p'_2 & \cdots & \bar{p}'_n p'_n & \bar{p}'_n \bar{p}'_1 & \bar{p}'_n \bar{p}'_2 & \cdots & \bar{p}'_n \bar{p}'_n \end{matrix}$$

The symbols A_{pq} , $B_{pq'}$, $C_{p'q}$ and $D_{p'q'}$ shall be used to represent an element in the respective sub-arrays \mathbf{A}_{pq} , $\mathbf{B}_{pq'}$, $\mathbf{C}_{p'q}$ and $\mathbf{D}_{p'q'}$. In the above expression of the vector-set array (1), the elements in the main diagonal naturally define the origin point, while those in the diagonals of sub-arrays $\mathbf{B}_{pq'}$ and $\mathbf{C}_{p'q}$ are the images based upon centrosymmetrical pairs of points. The diagonal images of $\mathbf{B}_{pq'}$ and $\mathbf{C}_{p'q}$ are therefore positive and single points.

In the sub-arrays images other than the diagonal elements are either positive or negative. Although they are single point in the above expression of sub-arrays, there exists, for each non-diagonal image, the other image which coincides to it. This is because in the fundamen-

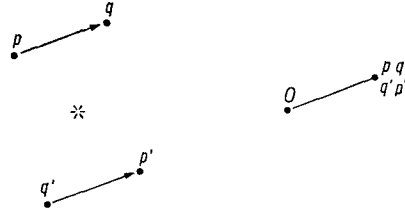


Fig. 1. Two centrosymmetrical pairs of points (*left*), showing the vector relating the points p and q , and that relating q' and p' give, in vector space, a double image (*right*)

tal set there are two pairs of points so arranged that the vector relating the points of one pair in the same way as the vector relating the points of the other (Fig. 1). The two vectors coincide in vector space, and the points at the ends of the vectors become in effect double points. The images which coincide to each other are given below:

$$\begin{aligned} A_{pq} &= D_{q'p'} \\ A_{qp} &= D_{p'q'} \end{aligned} \quad (2)$$

$$\begin{aligned} A_{pq} &= D_{q'p'} \\ A_{qp} &= D_{p'q'} \\ B_{pq'} &= B_{qp'} \\ B_{p'q} &= B_{q'p} \end{aligned} \quad (3)$$

$$\begin{aligned} C_{p'q} &= C_{q'p} \\ C_{p'q} &= C_{q'p} \end{aligned} \quad (4)$$

Since the vector-set array (1) is symmetrical about the main diagonal, there are further relations as shown below.

$$A_{pq} = -A_{qp}, \quad D_{p'q'} = -D_{q'p'} \quad (5)$$

$$B_{pp'} = -C_{p'p}, \quad B_{pq'} = -C_{q'p}, \quad B_{qp'} = -C_{p'q}. \quad (6)$$

These minus signs indicate inverse images, i.e. A_{pq} is inverse to A_{qp} . Image properties of the vector sets arisen from centrosymmetrical sets of positive and negative points will be discussed in the following by using the above representation of vector-set array.

Image properties

Consider, for simplicity, a centrosymmetrical set of eight points $a + b + \bar{c} + \bar{d} + a' + b' + \bar{c}' + \bar{d}'$, in which a', b', \bar{c}' , and \bar{d}' are the

points respectively related, by inversion, to a , b , \bar{c} , and \bar{d} . Then its vector-set array is given by

$$\begin{array}{cccc|cccc}
 \mathbf{V} = & aa & ab & a\bar{c} & a\bar{d} & aa' & ab' & a\bar{c}' & a\bar{d}' \\
 & ba & bb & b\bar{c} & b\bar{d} & ba' & bb' & b\bar{c}' & b\bar{d}' \\
 & \bar{c}a & \bar{c}b & \bar{c}\bar{c} & \bar{c}\bar{d} & \bar{c}a' & \bar{c}b' & \bar{c}\bar{c}' & \bar{c}\bar{d}' \\
 & \bar{d}a & \bar{d}b & \bar{d}\bar{c} & \bar{d}\bar{d} & \bar{d}a' & \bar{d}b' & \bar{d}\bar{c}' & \bar{d}\bar{d}' \\
 \hline
 & a'a & a'b & a'\bar{c} & a'\bar{d} & a'a' & a'b' & a'\bar{c}' & a'\bar{d}' \\
 & b'a & b'b & b'\bar{c} & b'\bar{d} & b'a' & b'b' & b'\bar{c}' & b'\bar{d}' \\
 & \bar{c}'a & \bar{c}'b & \bar{c}'\bar{c} & \bar{c}'\bar{d} & \bar{c}'a' & \bar{c}'b' & \bar{c}'\bar{c}' & \bar{c}'\bar{d}' \\
 & \bar{d}'a & \bar{d}'b & \bar{d}'\bar{c} & \bar{d}'\bar{d} & \bar{d}'a' & \bar{d}'b' & \bar{d}'\bar{c}' & \bar{d}'\bar{d}'
 \end{array} \tag{7}$$

The four parts divided by broken lines respectively correspond to the sub-arrays in the vector-set array (1). Thus, for example, according to the relations (2), $ba = a'b'$, or according to (4), $\bar{c}'b = b'\bar{c}$.

The feature characteristic of vector sets of sets of positive and negative unit points is the presence of single positive images based upon centrosymmetrical pairs of "negative" points, and that of negative double images. The study of the properties of these images is therefore of essential importance in the decomposition of vector sets under consideration.

Single positive images based upon pairs of negative points

Consider first an ordinary single positive image based upon a pair of positive points, say a and a' . Let it be chosen as the starting image and be connected to the origin. Then, as has been shown by BUERGER (1959), we obtain in vector space a set of eight line images parallel to the line image $aa + aa'$. This situation can be shown by connecting corresponding parts of the first and fifth columns of (7) as follows:

$$\begin{array}{l}
 a(a + a') \\
 b(a + a') \\
 \bar{c}(a + a') \\
 \bar{d}(a + a') \\
 a'(a + a') \\
 b'(a + a') \\
 \bar{c}'(a + a') \\
 \bar{d}'(a + a').
 \end{array} \tag{8}$$

Let the line $a + a'$ be denoted by A at its centre. Then the collection of the parallel line images (8) is expressed by

$$(a + b + \bar{c} + \bar{d} + a' + b' + \bar{c}' + \bar{d}') A = \mathbf{P}A, \quad (9)$$

in which \mathbf{P} represents the polygon as defined by the points in the parentheses, and corresponds to the image polygon which is to be solved.

Now, an image based upon a pair of negative points, say \bar{c} and \bar{c}' , is chosen, and it is connected to the origin to form a line image $\bar{c}\bar{c} + \bar{c}\bar{c}'$, we obtain, from the third and seventh columns of (7), the following set of parallel line images:

$$\begin{aligned} a(\bar{c} + \bar{c}') \\ b(\bar{c} + \bar{c}') \\ \bar{c}(\bar{c} + \bar{c}') \\ \cdot \\ \cdot \\ \cdot \\ \bar{d}'(\bar{c} + \bar{c}'). \end{aligned} \quad (10)$$

Since, for example, the negative line image $a(\bar{c} + \bar{c}')$ is expressed by $\bar{a}(c + c')$ (TAKÉUCHI, 1972), (10) can be rewritten by

$$\begin{aligned} \bar{a}(c + c') \\ \bar{b}(c + c') \\ c(c + c') \\ \cdot \\ \cdot \\ \cdot \\ \bar{d}'(c + c'). \end{aligned} \quad (11)$$

If the line $c + c'$ is likewise represented by C , (11) is rewritten by

$$(\bar{a} + \bar{b} + c + d + \bar{a}' + \bar{b}' + c' + d') C = \mathbf{P}'C. \quad (12)$$

Comparing (9) and (12), we notice that $\mathbf{P}' = -1 \times \mathbf{P}$. The image polygon \mathbf{P}' thus corresponds to the negative polygon of \mathbf{P} . Using the notation given by TAKÉUCHI (1972), this relation is expressed by $\mathbf{P}' = \bar{\mathbf{P}}$. Consequently, if a vector set is solved based upon the image arisen from a centrosymmetrical pair of negative points, the solution results which is related to the true solution by anti-inversion operation. For the convenience of subsequent discussions, the positive

single images based upon centrosymmetrical pairs of positive points will be denoted by $I(pp)$, and those based upon centrosymmetrical pairs of negative points by $I(nn)$.

In the cases of superstructures which are produced by adding atoms in basic structures, $I(pp)$ and $I(nn)$ have different weights. For example, if a superstructure in this category has a multiplicity m , the positive densities in its $\delta(x)$ are weighted by $(m - 1)/m$, while negative ones by $1/m$. It follows that the image points $I(pp)$ are weighted by $(m - 1)^2/m^2$, whereas $I(nn)$ by $1/m^2$. This difference will in principle serve for distinguishing $I(pp)$ from $I(nn)$, except for the case of $m = 2$. For this specific case of $m = 2$, both $I(pp)$ and $I(nn)$ have in general the same weight. Since, however, for such a case of superstructure, $\delta(x)$ itself has an antitranlation, no practical difficulty arises; irrespective of whether we choose $I(pp)$ or $I(nn)$ as starting images to decompose vector sets. We shall come to discuss this point later (p. 327).

Negative images

In general cases in which fortuitous overlappings of images do not occur, the negative images in the vector sets arisen from sets of positive and negative points are always doubled. For centrosymmetrical crystals, the centrosymmetrical pair of a pair of positive and negative points forms in vector space a pair of linear sets of three images, which have been called by TAKÉUCHI (1972) linear quadrup-

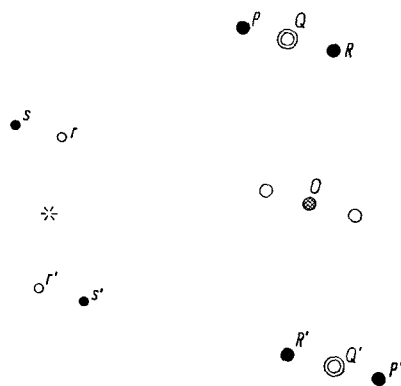


Fig.2. A pair of linear quadruple sets of images $\{P (= s's), Q (= r's + s'r) R (= r'r)\}$ and $\{P', Q', R'\}$ (right) given by two centrosymmetrical pairs of points in the left. Solid and open circles respectively represent positive and negative points

lets (Fig. 2). An inversion image $I(pp)$ occurs at one end of a linear quadruplet, and $I(nn)$ at the other end of the linear quadruplet; at its centre, two negative images occur, giving a negative double image. Therefore, by locating such a linear set of images, each having proper weight, the location of $I(pp)$ or $I(nn)$ can readily be identified.

However, one should not choose negative images as the starting images of vector-set decomposition. Should we use them, there arises a difficulty as shown in the following. Suppose that a negative image $b\bar{c}$ is connected to the origin to form the line $b\bar{b} + b\bar{c}$. Then, from corresponding parts of the second and third columns of (7), a set of eight line images parallel to $b(b + \bar{c})$ results.

Since, according to the relation (2), $b\bar{c} = \bar{c}'b'$, the above procedure inherently yields the other set of line images parallel to $b'(b' + \bar{c}')$. They are shown below:

$$\begin{array}{rcl}
 a(b + \bar{c}) & & a(b' + \bar{c}') \\
 b(b + \bar{c}) & \text{---} & b(b' + \bar{c}') \\
 \bar{c}(b + \bar{c}) & \text{---} & \bar{c}(b' + \bar{c}') \\
 \bar{d}(b + \bar{c}) & \text{---} & \bar{d}(b' + \bar{c}') \\
 a'(b + \bar{c}) & & a'(b' + \bar{c}') \\
 b'(b + \bar{c}) & \text{---} & b'(b' + \bar{c}') \\
 \bar{c}'(b + \bar{c}) & \text{---} & \bar{c}'(b' + \bar{c}') \\
 \bar{d}'(b + \bar{c}) & & \bar{d}'(b' + \bar{c}').
 \end{array} \tag{13}$$

In the above sets of line images, the images which coincide are tied together. It should be noted in (13) that each of these line images, unlike those of (8) and (10), is defined by one positive point image at one end of the line and one negative point image at the other end. It follows that if an image-seeking function is applied based upon a negative image like $b\bar{c}$, superpositions of positive and negative images occur in the procedure of forming this function, thus causing a complexity in interpreting the result. In general, the superposition of this sort never occur if we so far use positive images to form image-seeking functions.

Multiple images

The penalty for choosing a multiple peak for forming a line to be used as a first image is to incur a multiple solution (BUERGER, 1959). Except unavoidable cases like terramycin hydrochloride (TAKÉUCHI

and BUERGER, 1960) whose Patterson does not have single images based upon heavy atoms owing to their specific locations in the unit cell, straightforward decomposition of a vector set indeed depends on a successful choice of an initial image having single weight. Since partial Pattersons are, like ordinary Pattersons, continuously varying functions, peaks may be multiple owing to fortuitous chance of coincidence of two or more peaks, or by symmetry operations. It is thus desirable to look into the properties of multiple images characteristic of partial Pattersons. In addition to the coincidences of images of the same sign as in ordinary Pattersons, two types which are particular to partial Pattersons are the following:

1. Coincidence of the two different types of single images, $I(pp)$ and $I(nn)$.

Suppose in the vector-set array (7), $aa' = \bar{c}\bar{c}'$. Then by connecting this multiple image to the origin, we obtain the following set of sixteen parallel line images.

$$\begin{array}{ll}
 a(a+a') & \text{---} \\
 b(a+a') & \text{---} \\
 \bar{c}(a+a') & \text{---} \\
 \bar{d}(a+a') & \text{---} \\
 a'(a+a') & \text{---} \\
 b'(a+a') & \text{---} \\
 \bar{c}'(a+a') & \text{---} \\
 \bar{d}'(a+a') & \text{---} \\
 a(\bar{c}+\bar{c}') & \text{---} \\
 b(\bar{c}+\bar{c}') & \text{---} \\
 \bar{c}(\bar{c}+\bar{c}') & \text{---} \\
 \bar{d}(\bar{c}+\bar{c}') & \text{---} \\
 a'(\bar{c}+\bar{c}') & \text{---} \\
 b'(\bar{c}+\bar{c}') & \text{---} \\
 \bar{c}'(\bar{c}+\bar{c}') & \text{---} \\
 \bar{d}'(\bar{c}+\bar{c}') & \text{---}
 \end{array} \quad (14)$$

The line images which coincide are tied together. Obviously from this, two image polygons PA and $P\bar{C}$ ($=\bar{P}C$) are formed. Thus, we can describe this situation as follows: when two types of single images $I(pp)$ and $I(nn)$ coincide in a vector set, the result of decomposition of the vector set based upon the multiple image is a multiple of positive and negative solutions. An example of such a multiple solution is illustrated in Fig. 3 using a one-dimensional periodical array of circles.

2. Coincidence of positive and negative images.

Because of the reason given later, negative images have, except for the purpose of locating initial images of single weight, less practical importance in actual procedure of vector-set decomposition. The cases,

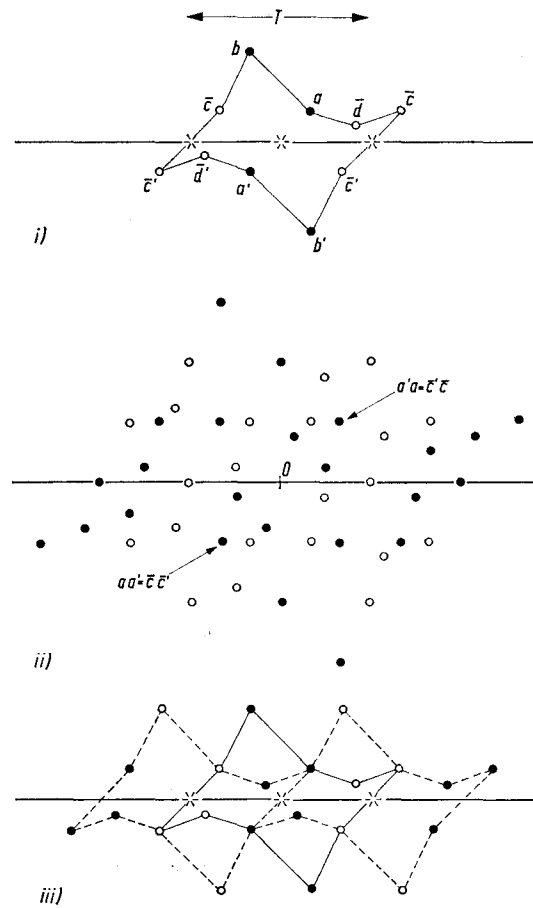


Fig. 3. An example of multiple solution based upon a multiple image composed of a centrosymmetrical pair of positive points and that of negative points. (i) A fundamental set of points, in which $a'a = \bar{c}'\bar{c}$. This set represents the unit of a linear periodic set of points. (ii) The vector set of the fundamental set (i). The multiple images are indicated. (iii) The solution of the vector set (ii) based upon the multiple images $a'a (= \bar{c}'\bar{c})$, showing resulting multiple image polygons.

Solid and open circles respectively indicate positive and negative points

however, which may be worth mentioning are those in which coincidence of positive and negative peaks still gives a residual positive peak. If such a multiple positive peak is erroneously chosen for forming a line to be used as an initial image, superpositions of positive and negative peaks occur in the process of forming image-seeking functions based upon the line image. This is because, by forming the line image,

a set of line images results which consists of line images like those of (13) in addition to the line images like those of (8) or (10).

Since multiplicity of a peak can be judged by calibrating volumes expected for single peaks, any confusion which may arise by choosing the multiple peaks as initial images can be avoided.

Procedure of decomposition

The partial Patterson of a superstructure is, as already mentioned, the self-convolution of the difference electron density $\delta(x)$, the difference between the real electron density of the superstructure and the electron density corresponding to the structure averaged over all its subcells. Since $\delta(x)$ is a function having positive and negative values, to solve a partial Patterson function for its $\delta(x)$, we have to, in principle, take account of negative values as well as positive. In fact, in the difference electron density of a superstructure caused by a simple ordering of different kinds of atoms, like Cu and Fe in chalcopyrite CuFeS_2 , positive densities represent the positions of atoms whose densities are higher than the average of the atoms involved in the ordering process, and negative ones represent those of atoms whose densities are smaller than the mean value. Therefore, negative peaks in the partial Patterson of such a structure bears a significant importance. However, as has been discussed by TAKÉUCHI (1972) elsewhere, in general cases of superstructures arisen by displacement or addition of atoms in a basic structure, negative peaks in $\delta(x)$ do not necessarily represent the atomic positions corresponding to complementary structure, the part of superstructure which is responsible for giving superstructure reflections. Only positive part of $\delta(x)$ represents the real electron density corresponding to a complementary structure. Thus in the practice of interpreting partial Pattersons, in general, we may disregard negative peaks once single positive peaks are found, as initial images, utilizing geometrical relations among positive and negative peaks specific to a given crystal symmetry (TAKÉUCHI, 1972).

In general, the vector set formed by a set of n positive and n' negative points has excess $n'(n' - 1)$ positive images compared to that arisen from a set of n positive points only. It follows that the partial Patterson of a difference electron density $\delta(x)$ which contains n positive peaks has more fortuitous chance of overlapping of positive peaks than the ordinary Patterson of a crystal having n atoms in the unit cell. Consequently, if a pair of atoms $\partial\rho(x_a)$ and $\partial\rho(x_b)$ in the

difference density $\delta(x)$ of a centrosymmetrical crystal gives a peak $P_2(x_a - x_b)$ in its partial Patterson, the following relation will hold

$$P_2(x_a - x_b) \geq 2 \partial \rho(x_a) \cdot \partial \rho(x_b). \quad (15)$$

The scale factor 2 in the above relation means that the atoms of the pair are not related by the centre of symmetry. However, in partial Pattersons there may also be a possibility that certain positive peaks overlap with negative peaks. Should it occur, the partial Patterson peaks may not hold the relation (15), but may have smaller weight. We should always bear this situation in mind.

The relation (15) is parallel with that between electron density and ordinary Patterson function. Thus automatic search of image locations in partial Pattersons will be most effectively performed by the method of minimum functions. The general procedure of interpreting partial Pattersons can now be summarized as follows: Prepare partial Patterson maps containing negative contours, and find, in the maps single positive images utilizing geometrical relations among positive and negative peaks specific to a given crystal symmetry. Then apply to the positive parts of the partial Pattersons the minimum-function method based upon the images. In this image-seeking procedure, negative parts of the functions may be in general treated as parts of the functions having zero value.

The real negative atoms

The partial Patterson method can readily be applied to the interpretation of certain Pattersons based upon neutron-diffraction intensities. For neutron diffraction, the nuclei of some of the atoms like Mn, Ti and V have negative diffraction amplitudes. Therefore these atoms can be regarded, for neutron diffraction, as "*negative atoms*". If a crystal contains negative atoms, the Fourier synthesis using structure factors derived from the neutron-diffraction data of the crystal yields negative peaks corresponding to the atoms. The negative peaks in the Fourier map are by no means spurious but represent real existing negative atoms. In that event the Patterson map of the crystal gives negative peaks based upon pairs of negative and ordinary atoms. To interpret such a Patterson, the negative peaks evidently can not be neglected. The theory of vector sets of positive and negative unit points will naturally aid in locating positive single images in the Patterson.

Example

As examples of the decomposition of partial Patterson functions, the direct determinations of the crystal structures of sérandite and banalsite are described in the subsequent paragraphs.

Sérandite

This mineral is the manganese analogue of pectolite $\text{Ca}_2\text{NaHSi}_3\text{O}_9$, and has a strong quasi-periodicity of $\mathbf{b}/2$, suggesting a substructure of this periodicity. The structure of sérandite hence bears a superstructure relation to this substructure. As has been shown by BUERGER (1956) and PREWITT (1967) for pectolite, it is thought that the superstructure of sérandite also would have been arisen mainly by adding silicate chains, which have the periodicity of \mathbf{b} , to arrays of octahedra formed by oxygen atoms about cations which have the quasi-periodicity of $\mathbf{b}/2$. This moderately complex scheme of superstructure is suited for testing the general procedure of decomposing partial Pattersons.

The specimens of sérandite we used were from Tanohata mine, Japan, and kindly furnished by Prof. T. WATANABÉ. Electron microprobe analyses yielded the chemical composition



The triclinic unit cell has dimensions: $a = 7.683(1) \text{ \AA}$, $b = 6.889(1) \text{ \AA}$, $c = 6.747(1) \text{ \AA}$, $\alpha = 90.53(5)^\circ$, $\beta = 94.12(2)^\circ$, $\gamma = 102.75(2)^\circ$, and contains one formula unit. The space group $P\bar{1}$.

The intensities of 2043 reflections in total were measured with $\text{MoK}\alpha$ radiation on a four-circle automatic diffractometer. Although the reflections with $k = 2n + 1$ which correspond to the superstructure reflections are mostly very weak, 822 reflections out of possible 1027 superstructure reflections with $\sin \theta \leq 0.5$ were measured with counts significantly above background level. The partial Patterson $P_2(\mathbf{u})$ was then computed based upon these superstructure reflections alone.

In order to interpret this partial Patterson function, a search was first made of locating linear quadruplets of peaks, each of which is, as stated earlier, composed of two positive single peaks and one negative double peak between them. The multiplicity of peaks was predicted by calibrating peaks in comparison with the origin peak of the ordinary Patterson function of sérandite. Since the multiplicity of this superstructure is two, the j th atom \mathbf{r}_j in the difference function

$\delta(x)$ is in general weighted by $Z_j/2$. Therefore, a single peak in the partial Patterson should be weighted by $Z_j^2/4$. It is to be noted, however, that such an estimation of peak weights is valid only for peaks arisen by the atoms which have been added to the basic structure and responsible for the superstructure reflections. If, in general, slight displacements of atoms in the basic structure of a superstructure occur with respect to the corresponding locations in subcells, the weights of partial-Patterson peaks based upon these atoms are, related to the magnitude of the atomic displacements, atomic number and multiplicity.

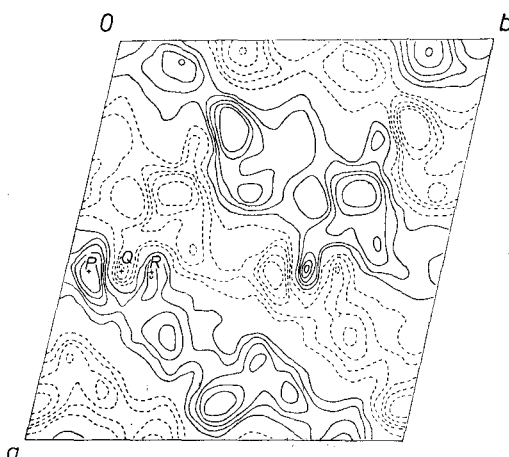


Fig. 4. The partial-Patterson section of the level $z = 0.32$. A linear quadruplet consisting of three peaks P , Q , and R is indicated. The positive peak P was used to form $\partial M_2(xyz)$

For the case of sérandite, the complimentary part of the structure, which is responsible for superstructure reflections, consists of Si, O, and Na atoms. A single peak in the partial Patterson is therefore expected to have the weight $kZ_{\text{Si}}^2/4$, $kZ_{\text{O}}^2/4$ or $kZ_{\text{Na}}^2/4$, where k is the calibration factor that places the peak heights upon an absolute basis; all of these are of similar value. Bearing this situation in mind, we immediately found several linear quadruplets in the partial Patterson of sérandite. Of these, one of the well defined ones was chosen (Fig. 4), and a minimum function $\partial M_2(xyz)$ was formed based upon one of the positive peaks of the linear quadruplet. Since there were, in this minimum function, still too many peaks, another minimum function

$\partial M'_2(xyz)$ was formed based upon a positive peak of another linear quadruplet. The both minimum functions thus formed have, if origins are properly chosen, similar characteristic features in the arrangements of peaks in the unit cells. They were then combined to form a minimum function of higher rank $\partial M_4(xyz)$. As shown in Fig. 5, $\partial M_4(xyz)$ was readily interpreted, and the approximate locations of silicon, sodium and oxygen atoms which belong to the complimentary structure were unambiguously determined.

In connection with the procedure given above, a mention should be made of the alternate solutions (TAKÉUCHI, 1972) based upon

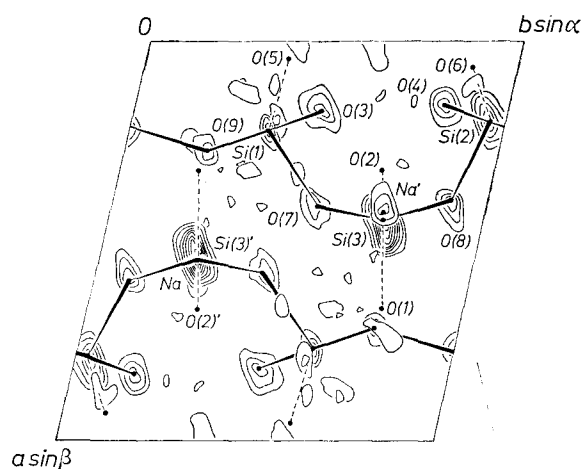


Fig. 5. A composite map of $\partial M_4(xyz)$. Final locations of Na, Si, O(3), O(4), O(7), O(8), and O(9) that form the complimentary structure are indicated. Those for O(1), O(2), O(5), and O(6), which are the substructure atoms (their peaks are hence missing in this map), are also given

a linear quadruplet. One of the positive peaks in a linear quadruplet is, as argued, given by a pair of negative atoms. If a minimum function is formed based upon such a positive peak, the result is the anti-centrosymmetrical image of the minimum function formed by the other positive image of the same linear quadruplet. However, for such a superstructure like sérandite that arises from a basic structure by doubling one of its axes, say b , the difference function $\partial(x)$ itself has an anti-translation of $b'/2$. It follows that the two alternate solutions, for this case, are related to each other simply by a translation of $b/2$. This situation is illustrated in Fig. 6. Therefore, in general,

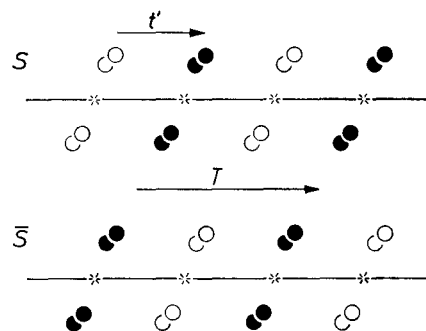


Fig. 6. A linear centrosymmetrical periodic set S of positive and negative points, and its negative set \bar{S} , showing that they are related to each other by an anti-translation t' ($t' = T/2$). Positive and negative points are respectively expressed by solid and open circles

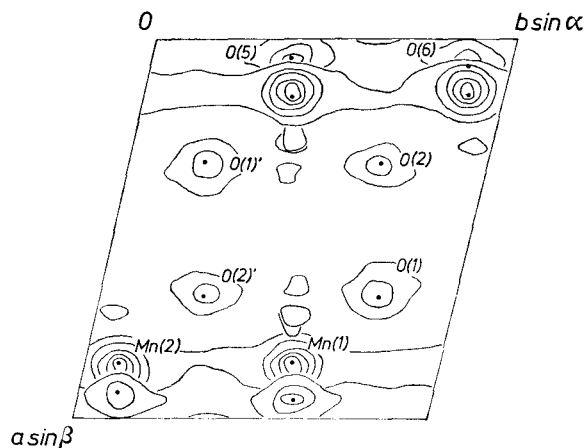


Fig. 7. $M_2(xyz)$ formed from the ordinary Patterson function of sérandite; only the peaks of atoms which are in the substructure are given

for this sort of superstructures, there is no practical difficulty due to the alternate solutions.

The locations of atoms in the subcells of sérandite were readily obtained from the ordinary Patterson (Fig. 7). From this result combined with that of $\partial M_4(xyz)$, we have now found the whole structure of sérandite (Fig. 8). The coordinates of atoms thus derived gave an $R = 0.35$. The structure has been refined to an $R = 0.034$ for 1766 observed reflections. The difference function $\partial(x)$ computed from hkl

reflections with $k = 2n + 1$ only is shown in Fig. 9, which is to be compared with $\partial M_4(xyz)$ as given in Fig. 5. Full details of the crystal structure of sérandite will be given elsewhere. A brief account on the

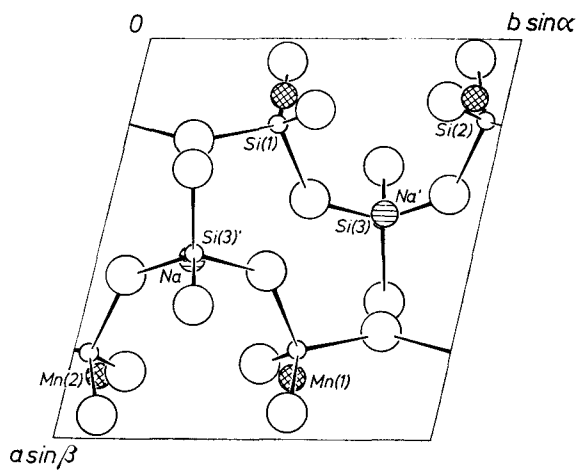


Fig. 8. The crystal structure of sérandite projected along the c axis

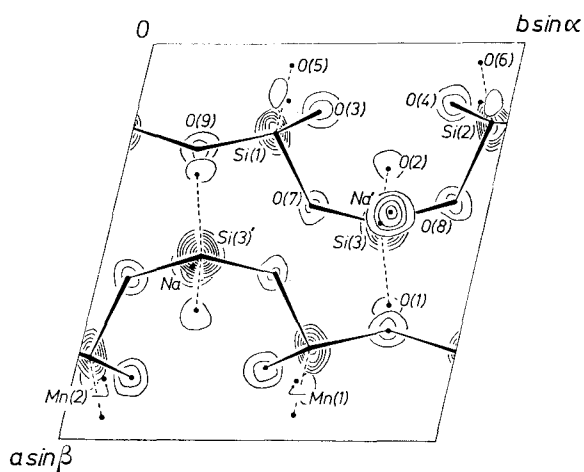


Fig. 9. Difference function $\delta(x)$ of sérandite. Note that smaller peaks corresponding to substructure atoms Mn(1), Mn(2), O(1) and O(2) occur in this map. This is because the distance between Mn(1) and Mn(2), and that between O(1) and O(2) are respectively slightly deviated from the substructure periodicity of $\mathbf{b}/2$

Table 1. *Atomic parameters of sérandite*
 Anisotropic temperature coefficients have been multiplied by 10^3 ; errors in the coefficients not indicated

Atom	x	y	z	β_{11}	β_{22}	β_{33}	β_{12}	β_{13}	β_{23}
Mn(1)	0.8527(1)	0.5943(1)	0.1363(1)	2.8	3.0	2.6	0.6	0.5	0.3
Mn(2)	0.8496(1)	0.0840(1)	0.1332(1)	2.2	2.9	2.1	0.9	0.3	-0.1
Na	0.5573(2)	0.2547(2)	0.3518(2)	3.8	8.6	6.3	1.0	1.0	-0.2
Si(1)	0.2166(1)	0.4025(1)	0.3414(1)	1.9	1.5	1.9	0.6	-0.3	-0.2
Si(2)	0.2071(1)	0.9526(1)	0.3506(1)	1.9	1.8	1.5	0.7	0.1	-0.2
Si(3)	0.4545(1)	0.7388(1)	0.1430(1)	1.3	2.4	1.5	0.3	0.2	0.2
O(1)	0.6641(3)	0.7953(4)	0.1147(4)	2.2	4.2	4.5	0.7	1.4	0.5
O(2)	0.3236(3)	0.7097(4)	-0.0569(4)	2.7	4.3	3.0	0.5	-0.2	-0.3
O(3)	0.1809(4)	0.4954(4)	0.5533(4)	5.7	3.7	3.4	2.9	0.9	-0.2
O(4)	0.1599(4)	0.8457(4)	0.5567(4)	5.5	3.2	3.3	1.2	1.4	0
O(5)	0.0609(3)	0.3905(4)	0.1684(4)	2.5	4.8	2.1	0.6	-0.2	0.3
O(6)	0.0530(3)	0.8932(4)	0.1727(4)	2.7	4.6	2.9	1.3	-0.6	-0.7
O(7)	0.4077(3)	0.5332(4)	0.2738(4)	2.7	3.8	3.7	0.8	0	1.8
O(8)	0.3973(3)	0.9052(4)	0.2879(4)	2.4	3.5	4.8	1.3	-0.1	-1.8
O(9)	0.2613(3)	0.1900(3)	0.3928(4)	3.8	2.6	4.1	0.8	0.1	0.2

hydrogen bonding in this structure has appeared (TAKÉUCHI and KUDOH, 1972). The final atomic coordinates are listed in Table 1.

Banalsite

Banalsite is an orthorhombic mineral which was described by SMITH, BANNISTER and HEY (1944) as a new barium-felspar. The intensities of x-ray diffractions of this mineral are, if $l = 2n + 1$, very weak, suggesting a substructure having the periodicity of $c/2$. The structure of banalsite thus bears a superstructure relation to this substructure. The partial-Patterson method was tested to the structure determination of banalsite in order to see the power of this method especially when it is applied to this sort of superstructures having higher symmetry.

The lattice constants determined by the use of a four-circle automatic diffractometer are: $a = 8.496(2)$ Å, $b = 9.983(2)$ Å, $c = 16.755(3)$ Å. The unit cell contains four formula units of $\text{BaNa}_2\text{Al}_4\text{Si}_4\text{O}_{16}$. The space group is $Ibam$, the centrosymmetric structure being confirmed by the $N(z)$ test. A total of 1074 independent reflections were measured up to $\sin \theta = 0.50$. A calculation shows that the average of the normalized structure factors $|E|$ for the superstructure reflections is 0.36, while that for the reflections with $l = 2n$ is 1.06. Because of such a big difference in intensities

between odd-order and even-order reflections in l neither the ordinary Patterson method nor statistical methods are of advantage to straightforward determination of the crystal structure of banalsite.

Determination of the average structure

The structure analysis was initiated by determining the average structure, or substructure, having the periodicity of $c/2$. To deal with average structures having higher symmetry like the present case, it is desirable to derive their symmetries first. This can be done by the use of the theory of derivative crystal structures given by BUERGER (1947), who showed the way to derive the symmetry of a derivative structure, or superstructure, from that of the basic structure from which the superstructure was derived. Since the symmetry relation between a superstructure and its basic structure is parallel to that of the superstructure and the structure averaged over all its subcells, we can derive, by following, in the reverse way, the result given by the BUERGER's theory, the symmetry of the average structure from that of a given superstructure. Thus we found the space group of the average structure of banalsite to be $Cbam$ whose standard notation is $Cmmm$.

Since the true unit cell contains only four barium atoms, they should be distributed over the set of special positions $(000, 00\frac{1}{2}, \frac{1}{2}\frac{1}{2}\frac{1}{2}, \frac{1}{2}\frac{1}{2}0)$ or $(00\frac{1}{4}, 00\frac{3}{4}, \frac{1}{2}\frac{1}{2}\frac{3}{4}, \frac{1}{2}\frac{1}{2}\frac{1}{4})$. These sets of special positions respectively correspond to those of the special positions $(000, \frac{1}{2}\frac{1}{2}0)$ and $(00\frac{1}{2}, \frac{1}{2}\frac{1}{2}\frac{1}{2})$ in the subcell. This situation immediately yields the probable sign of F_{hkL} in terms of the contributions of barium atoms, where L represents even number of l . Thus, by assigning a weight to each F_{hkL} , according to the probability (SIM, 1961) that the sign of F_{hkL} is the same as the sign of the contributions of barium atoms, a Fourier synthesis was evaluated to obtain the atomic locations in the substructure. As shown in Fig. 10, which shows the resulting Fourier map, all atoms are clearly resolved. The atomic locations thus obtained are in actual case composed of the set of true atomic locations and its mirror images due to the sets of mirrors parallel to (100) and (010) , which are both missing in the true structure.

Partial-Patterson map

In order to select, from the above result, the true set of atomic locations, the partial Patterson was then calculated using the superstructure reflections only. Since only odd-order terms in l are used

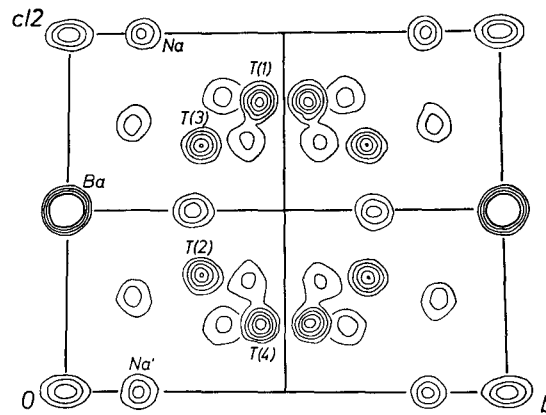


Fig. 10. Composite diagram of three-dimensional Fourier synthesis, showing the average structure of banalsite. Contours at equal intervals on an arbitrary scale. Peaks in the sections from $x = 0$ to $x = \frac{1}{4}$ are given

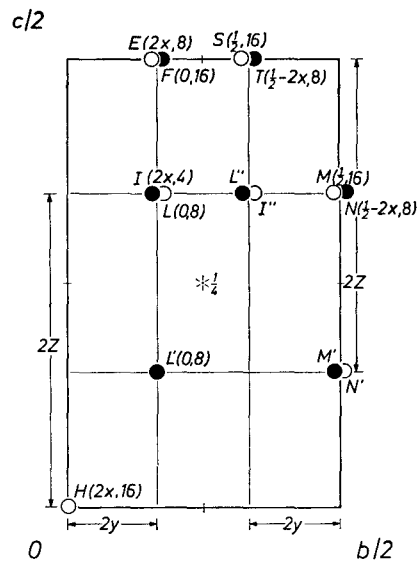


Fig. 11. Geometrical relationship between an inversion image I at $2x, 2y, 2z$, and its satellites characteristic of the vector set of a point set having the Shubnikov symmetry $I_c bam$. The vector set itself has the Shubnikov symmetry $I_c mmm$. The images indicated by letters with primes or double primes are respectively related, by the symmetry, to those indicated by corresponding letters. For each image, the height and multiplicity are indicated in this order in parentheses. Solid and open circles are respectively positive and negative images

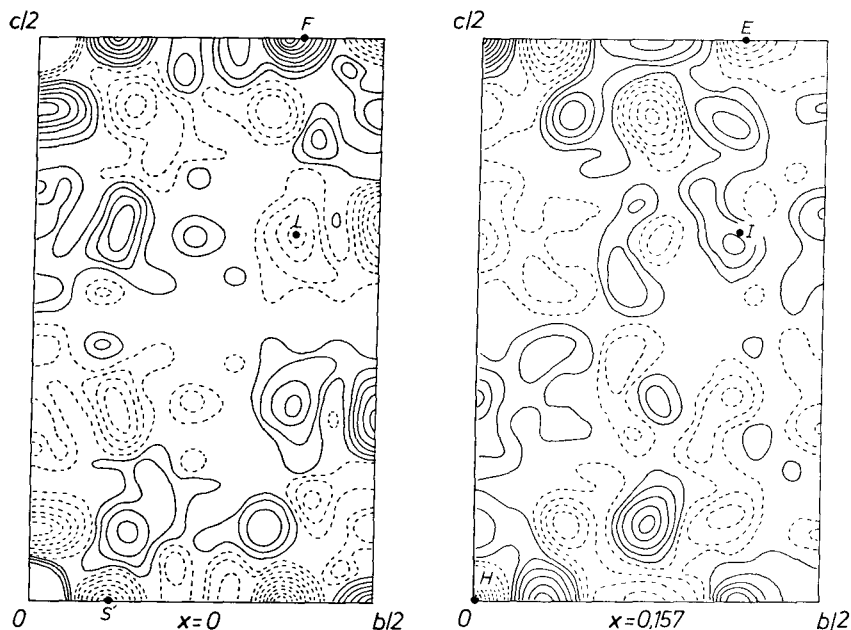


Fig. 12. Partial-Patterson sections, $x = 0$ and $x = 0.157$, of banalsite; an inversion image I , and some of its satellites are indicated. Broken contours indicate negative peaks

for this computation, the map displays an antisymmetry corresponding to the Shubnikov group $III_{71}^{538} - I_c mmm$ (KOPTSIK, 1966). The interpretation of this partial Patterson should be made, in the first place, with due regard to the symmetry of the difference function $\delta(x)$ of banalsite. This function also has an antitranslation having the magnitude of $c/2$. Therefore, by multiplying this antitranslation to the space group $Ibam$ of banalsite, we can obtain the space group for $\delta(x)$. This procedure may be shown by

$$\{Ibam\} \cdot \{c'/2\} \rightarrow \{I_c bam\}.$$

The resulting group of antisymmetry corresponds to the Shubnikov group III_{72}^{546} (KOPTSIK, 1966).

The distribution of positive and negative points in this space group defines, in vector space, a specific geometrical relation in the locations between inversion images and their satellites. Some representative satellites of an inversion image are graphically shown in Fig. 11. As will be observed in Fig. 11, the presence of negative satellites in addition to positive highly secures the correct choice of inver-

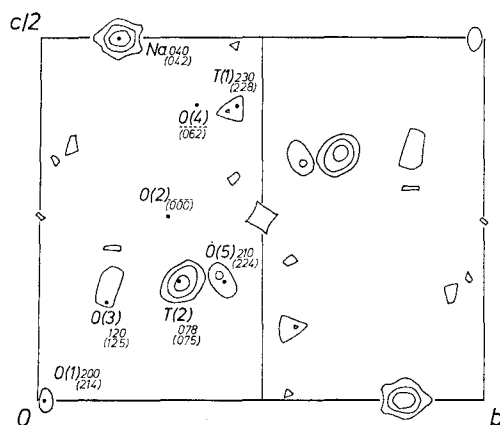


Fig. 13. $\partial M_2(xyz)$ based upon the image *I* as shown in Fig. 12; peaks in the sections from $x = 0$ to $x = \frac{1}{4}$ are given. Final atomic locations are indicated by dots. Numbers give in decimal fractions of the a length the height of peaks; those in parentheses the height of final atomic locations

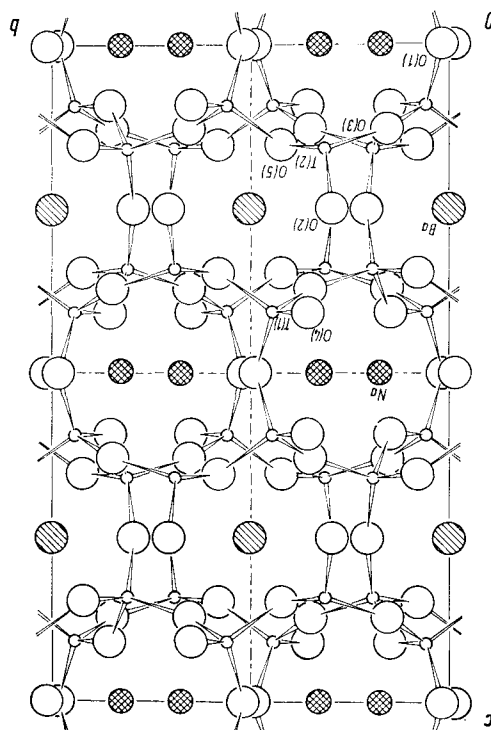


Fig. 14. The a -axis projection of the crystal structure of banalsite

Table 2. *Atomic parameters of banalsite*
 Anisotropic temperature coefficients have been multiplied by 10^3

Atom	x	y	z	β_{11}	β_{22}	β_{33}	β_{12}	β_{13}	β_{23}
Ba	0.0000	0.0000	0.2500	3.45	1.67	0.69	0	0	0
Na	0.0422(4)	0.1745(4)	0.5000	4.75	2.67	1.41	0.57	0	0
T(1)	0.2283(2)	0.4429(2)	0.4067(1)	2.10	1.01	0.29	-0.38	0.07	-0.05
T(2)	0.0754(2)	0.3095(2)	0.1586(1)	2.54	2.06	0.62	-0.21	0.13	-0.03
O(1)	0.2143(7)	0.0153(6)	0.0000	2.65	4.18	0.56	0.20	0	0
O(2)	0.0000	0.2928(6)	0.2500	5.42	2.62	0.89	0	-0.32	0
O(3)	0.1255(5)	0.1532(4)	0.1287(3)	2.55	1.29	1.39	1.16	0.37	-0.06
O(4)	0.0618(6)	0.3534(4)	0.4082(3)	5.46	1.63	0.81	-0.54	0.31	-0.32
O(5)	0.2238(5)	0.4213(4)	0.1535(3)	2.14	2.93	1.07	-1.25	0.29	0.20

sion images. For this specific set of symmetries under consideration the linear quadruplet based upon a centrosymmetrical pair of positive points and that of negative points necessarily occurs parallel to the a axis.

Using the above geometrical relation between inversion images and their satellites, an inversion image was in fact readily identified in the partial-Patterson map of banalsite. Then, based upon it, a minimum function $\partial M_2(xyz)$ was formed. The partial-Patterson sections which contain the inversion image and some of its satellites are shown in Fig. 12, and $\partial M_2(xyz)$ in Fig. 13. A comparison between $\partial M_2(xyz)$ and the average structure as shown in Fig. 10 has now revealed that Na, T(1), and T(2) are the true atoms of the banalsite structure. The true locations for some of the oxygen atoms are also found in $\partial M_2(xyz)$, but some are missing. Nevertheless, by taking account of bond lengths, the locations of T(1) and T(2) thus found immediately permit us to construct, in the average structure, the true framework of the banalsite structure. In $\partial M_2(xyz)$, we notice that the peak for T(1) is smaller than that for T(2). A study of the partial-Patterson map showed that this was caused by coincidence of positive and negative peaks due to interatomic vectors in which the T(1) atom is involved. The missing oxygen atoms in $\partial M_2(xyz)$ are in the similar situation.

The structure thus derived has been refined to an $R = 0.038$. The a -axis projection of the structure is illustrated in Fig. 14. To aid in constructing a three-dimensional view from this projection, the atomic coordinates are given in Table 2. Full details of the structure will be reported at a later date.

We are grateful to Prof. R. SADANAGA for his useful discussions, and to Prof. T. WATANABE for putting specimens of sérandite and banalsite at our disposal. Our special thanks are due to Prof. Y. ITAKA for his help in collecting counter intensity data at his laboratory. Dr. T. OZAWA and Dr. F. P. OKAMURA assisted in computation which was performed at the Computer Center of the University of Tokyo.

References

- M. J. BUERGER (1947), Derivative crystal structures. *Journ. Chem. Physics* **15**, 1–16.
- M. J. BUERGER (1956), The determination of the crystal structure of pectolite, $\text{Ca}_2\text{NaHSi}_3\text{O}_9$. *Z. Kristallogr.* **108**, 248–262.
- M. J. BUERGER (1959), *Vector space*. John Wiley and Sons, New York.
- V. A. KOPTSIK (1966), *Shubnikov groups*. Moscow University.
- C. T. PREWITT (1967), Refinement of the structure of pectolite, $\text{Ca}_2\text{NaHSi}_3\text{O}_9$. *Z. Kristallogr.* **125**, 298–316.
- G. A. SIM (1961), *Computing methods and the phase problem in x-ray crystal analysis*. Edit. by R. PEPINSKY, J. M. ROBERTSON and J. C. SPEAKMAN, 227–235. Pergamon Press, Oxford.
- W. CAMPBELL SMITH, F. A. BANNISTER and MAX H. HEY (1944), Banalsite, a new barium-felspar from Wales. *Mineral. Mag.* **27**, 33–46.
- Y. TAKÉUCHI (1972), The investigation of superstructures by means of partial Patterson functions. *Z. Kristallogr.* **135**, 120–136.
- Y. TAKÉUCHI and M. J. BUERGER (1960), The crystal structure of terramycin hydrochloride. *Proc. Nat. Acad. Sci.* **46**, 1366–1370.
- Y. TAKÉUCHI and H. HORIUCHI (1972), The application of the partial Patterson method and the thirteenfold hexagonal superstructure of $\text{Cu}_7\text{As}_6\text{Se}_{13}$. *Z. Kristallogr.* **135**, 93–119.
- Y. TAKÉUCHI and Y. KUDOH (1972), Valence balance of hydrogen-bonded systems in certain rock-forming silicates. *Acta Crystallogr. A* **28**, S 66–67.